Published in Journal of Applied Physics 90, issue 8, 3925-3933, 2001
which should be used for any reference to this work

Switchable yttrium–hydride mirrors grown on $CaF_2(111)$: A x-ray photoelectron spectroscopy and diffraction study

J. Hayoz[a)]
Institut de Physique, Université de Fribourg, Pérolles, CH-1700 Fribourg, Switzerland

J. Schoenes[b)]
Institut für Halbleiterphysik, Technische Universität Braunschweig, Mendelssohnstrasse 3, D-38106 Braunschweig, Germany

L. Schlapbach and P. Aebi
Institut de Physique, Université de Fribourg, Pérolles, CH-1700 Fribourg, Switzerland

The epitaxial growth of Y (hydride) films on $CaF_2(111)$ has been investigated using x-ray photoelectron spectroscopy, x-ray photoelectron diffraction, and low energy electron diffraction (LEED). For Y deposition at 700 °C the formation of high-quality epitaxial hcp(0001) oriented Y films is observed. Whenever the Y films showed good surface quality, the surface is rich in F. Only when the deposition temperature was chosen so low that the LEED reflexes were very broad was no fluorine detected. This is a strong indication that F acts as a surfactant. For Y deposition at room temperature under a H_2 partial pressure of 5×10^{-6} mbar we observe the formation of a F-free, transparent $YH_{2.3}$ film of a red/yellow color and poor crystallinity. Hydrogen unloading is accomplished by annealing to 600 °C. The film loses its transparency, the poorly ordered fcc(111) lattice converts to a well-ordered hcp(0001) lattice, and F contamination is restored.

I. INTRODUCTION

For decades the interaction of hydrogen with Y, La, and the rare-earth (RE) metals has been the subject of numerous investigations due to the interesting temperature- and concentration-dependent structures and properties observed in the solid solution (α phase) as well as in the stable dihydride (β) and trihydride (γ) phase.[1] Hydrogen induced metal–insulator transitions in REH_x as x approaches 3, for instance, have already been indicated by electrical transport measurements and (inverse) photoemission experiments on *bulk* samples in the 1980s.[1–3] Renewed interest in these phenomena has been developed by the recent discovery of spectacular changes in the optical properties of metal–hydride *films* of Y, La, and RE hydrides near their metal–insulator transition: in the metallic dihydride phase these layers appear mirrorlike, whereas the insulating trihydride phase is transparent for visible light.[4,5] As the transition from the shiny to the transparent state is reversible and induced at room temperature (RT) by simply changing the surrounding hydrogen gas pressure[4] or electrolytic cell potential,[6] these hydrides can be used as *switchable mirrors*.[7] In the transparent state they have characteristic colors: YH_3 is yellowish,[8] while LaH_3 is red. Even more spectacular are the optical changes of magnesium–gadolinium[9] and magnesium–yttrium alloys since they switch from metallic to colorless transparent during hydrogen absorption. This enhances their technological potential tremendously.

For basic research the intriguing questions are: what is the electronic structure of the insulating phase and what causes the phase transition? Three kinds of models have been proposed to account for the measured gap of 2.8 eV in YH_3. The local density approximation (LDA) of density–functional theory incorrectly gives a metallic state[10–14] unless a distortion of the HoD_3 structure is assumed.[13] This broken symmetry structure, which is only slightly more stable than the HoD_3 structure, has a LDA gap of only 0.8 eV. There has been a controversy as to whether the structure is consistent with neutron diffraction data.[15,16] Very recent Raman effect measurements[17] exclude the HoD_3 structure for YH_3 put forward by the early neutron data. Instead a noncentrosymmetric structure like $P6_3cm$ or $P6_3$ is compatible with the Raman data. To reconcile the small gap of a few tenth of an eV with the large transparency window over the visible spectral range observed in experiments[4,8,18] it has been argued that the theoretical gap is an indirect gap and that the experiment does not show zero absorption. It is not yet clear whether this residual absorption is, indeed, characteristic for YH_3 or whether it comes from the Pd cap layer which protects the Y film against oxidation during *ex situ* optical experiments. The second group consists of strongly correlated electron models.[19–21] Energy gaps of several eV can be obtained, depending on the Coulomb correlation energy. The third group, finally, deals with GW quasiparticle calculations.[22,23] A very recent study[23] predicts a fundamental gap of 1 eV and, taking into account electric dipole matrix elements, a large optical gap between 2.4 and 2.9 eV.

[a)]Present address: Department of Physics, Pennsylvania State University, PA 16802. Electronic mail: joh4@psu.edu
[b)]Author to whom correspondence should be addressed; work performed while on sabbatical at Institut de Physique, Université de Fribourg, Pérolles, CH-1700 Fribourg, Switzerland; Electronic mail: j.schoenes@tu-bs.de

An interesting feature of the latter two groups of models is that they predict that hydrogen is present as a negatively charged H^- ion.[19–21,23] This theoretical result is corroborated experimentally by Y $3d$ core-level shifts toward higher binding energies when going from Y to Y trihydride,[2,3,24–26] ion migration experiments,[27] and, very recently, by optical infrared spectroscopy.[28] According to Osterwalders Y $3d$ core-level shift analysis[3] 0.19 and 0.29 unit charges are transferred to each hydrogen in Y dihydride and Y trihydride, respectively. In the optics experiment infrared active optical phonons were excited in YH_3, which is only possible if electric dipole moments are present.[28] Since Y is certainly not negatively charged, it is the hydrogen that has to carry the negative charge in the partly ionic compound. Hjovarsson soft x-ray emission and absorption spectroscopy data[29] finally are interpreted in terms of H plus. This contradicts the conclusions from several other techniques, like x-ray photoelectron spectroscopy (XPS), ion migration, and infrared spectroscopy. While the first technique is very surface sensitive, the other two measure bulk properties, so that the argument that the difference might be due to the fact that XPS and soft x-ray absorption probe different parts of the sample does not hold.

A combination of photoemission[25,30] and inverse photoemission data could test the size of the fundamental gap. The key experiment to be done for the quantitative verification of the optical gap is a precise absorption measurement at the absorption edge on a *single-crystalline* sample containing no absorbing material other than YH_3. Due to the large volume expansion on loading with hydrogen Y hydride bulk samples decay into powders when approaching the trihydride phase[1] and, hence, are not suited for precise absorption measurements. Thin films, in contrast, can accommodate the volume changes upon loading and unloading by an expansion and a contraction perpendicular to the film plane, in particular, if the films are textured with the c axis of the hexagonal-closed packed (hcp) Y lattice oriented parallel to the growth direction.

While single-crystalline Y hydride films had previously been prepared on nontransparent W(110) substrates[24–26] and (11.0) oriented sapphire substrates covered with a (110)-oriented niobium buffer layer,[31–33] it was only recently found that epitaxial Y films can be grown without a buffer layer on transparent (111)-oriented CaF_2 substrates[34] and (111)-oriented BaF_2 substrates.[35] Indeed, crystals with the fluoride structure consist of three intercalated face-centered cubic (fcc) lattices and, hence, present suitable (111) surfaces for the growth of closed-packed Y layers. The lattice parameter a of CaF_2 is 5.45 Å, giving a cation nearest neighbor separation $d=a/\sqrt{2}=3.85$ Å. The separation of the Y atoms in the basal plane amounts to 3.65 Å, resulting in a lattice mismatch for the growth of Y on CaF_2 of 5.5%.

The possibility of growing high-quality epitaxial Y films on $CaF_2(111)$ without a buffer layer opens new possibilities to investigate single crystalline switchable mirrors. Especially for electrical resistivity and optical transmission experiments, the transparency of CaF_2 and its insulating nature are great advantages. However, beyond fundamental experiments this progress also offers new technological research opportunities. Given the compatibility with Si, optoelectronic applications might be envisaged.[34] Second, $Ca_{1-x}Y_xF_{2+x-y}H_y$ is a negative H ion conductor,[34] providing a promising alternative for gas phase[4] and wet electrochemical loading[6] for switchable mirror applications.

The question whether high-quality epitaxial Y(0001) films grown on $CaF_2(111)$ without a buffer layer are free of fluorine contamination is of importance for fundamental experiments as well as potential applications. Therefore we studied the growth process of Y on (111) oriented CaF_2 substrates with the combination of XPS, x-ray photoelectron diffraction (XPD), and low energy electron diffraction (LEED). Our results demonstrate that the growth of high-quality epitaxial Y(0001) films on $CaF_2(111)$ without a buffer layer is inseparable from the occurrence of fluorine. Moreover, we find remarkable differences to the growth process on W(110) for Y deposition under a hydrogen partial pressure: surprisingly, the hydrogen concentration of the resulting Y hydride films at a given hydrogen partial pressure is significantly larger for deposition on $CaF_2(111)$ than for deposition on W(110).

II. EXPERIMENTAL PROCEDURES

We used XPD to observe, in real space and near the surface, the changes occurring due to the H-induced structural transitions in yttrium. XPD has been chosen because of its chemical sensitivity and its sensitivity to local real-space order. LEED, in contrast, shows the symmetry of reciprocal space, is not chemically selective, and contains information about the long-range order of the atoms near the surface. XPD is a powerful technique for surface structural investigations,[36] and it has been shown that full hemispherical XPD patterns provide very direct information about the near-surface structure.[24–26,37–42] At photoelectron kinetic energies above about 500 eV, the strongly anisotropic scattering by the ion cores leads to a forward focusing of the electron flux along the emitter–scatterer axis. The photoelectron angular distribution, therefore, is to a first approximation a forward-projected image of the atomic structure around the photoemitters. Note that the cross section for forward scattering increases with increasing atomic number.[43] Therefore, forward scattering due to H atoms is generally too weak to be observed.

The XPD data are presented in so-called diffractograms, i.e., in a stereographic projection and in a linear gray scale image with maximum intensity corresponding to white (see Fig. 3). The center of the plots corresponds to the surface normal (polar emission angle $\Theta=0°$) while the outer circle represents directions parallel to the surface ($\Theta=90°$).

The experiments were performed in a Vacuum Generators ESCALAB Mk II Spectrometer modified for motorized sequential angle-scanning data acquisition,[37,38] equipped with a three-channeltron hemispherical electrostatic energy analyzer and with a base pressure in the low 10^{-11} mbar region. XPS and diffraction patterns were measured using Mg $K\alpha$ radiation ($h\nu=1253.6$ eV) with the sample kept at RT. The overall energy resolution is approximately 1 eV. The spectrometer is extended with an ultrahigh vacuum (UHV)

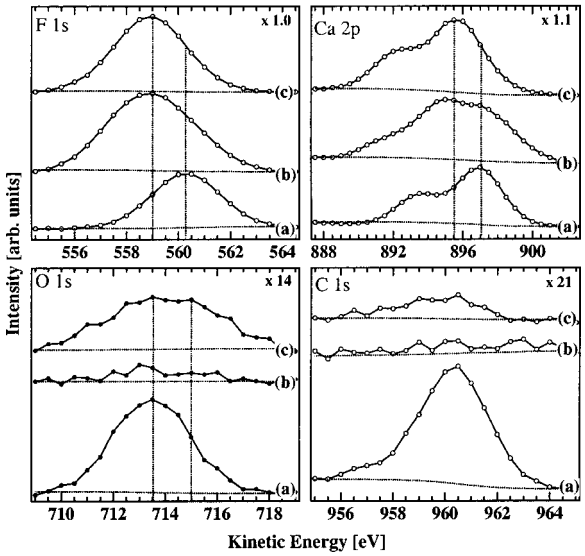

FIG. 1. XPS spectra taken from the (111) oriented CaF_2 substrate: (a) untreated, (b) after annealing to 700 °C for 30 min, and (c) after 20 h irradiation with photons ($h\nu = 1253.6$ eV) and photoelectrons ($E_{kin} \leq 1253.6$ eV) under UHV conditions. Due to the insulating nature of CaF_2 there is a charging effect which, compared to literature values for F 1*s* (≈569 eV) and Ca 2*p* (≈905.6 eV) in CaF_2, shifts the F 1*s* and Ca 2*p* emission by about 7 eV to lower kinetic energies.

compatible hydrogenation system.[26] In brief, it combines a high-pressure reaction cell with a custom made hydrogen purification system based on a Pd–24%Ag tube and a sorption pump. The hydrogen purification system removes residual contaminations from 6N–H_2 efficiently.[26]

The substrates were commercial (111) oriented, air-cleaved and polished 10 mm × 10 mm × 1 mm large CaF_2 platelets with a surface roughness of 2–3 Å. Due to the insulating nature of CaF_2 there is a charging effect which, compared to literature values for CaF_2,[44] shifts the XPS spectra from the bare CaF_2(111) substrate toward lower kinetic energies (Fig. 1). Prior to Y deposition the CaF_2 platelets were cleaned upon annealing to 700 °C (see Fig. 1). High purity Y (99.99%) was evaporated from a liquid nitrogen cooled electron-bombardment cell at different substrate temperatures with the pressure remaining below 2×10^{-10} mbar or under a hydrogen partial pressure of 5×10^{-6} mbar. During Y deposition the film thickness was controlled by means of a water-cooled quartz microbalance. The evaporation rate was typically 5–10 Å/min. Several LEED patterns were taken during and/or after the growth of the films and the annealing steps. Line shape and peak position of the Y 3*d* doublet, the F 1*s*, as well as the O 1*s* core level were probed with XPS. Finally, Y $3d_{5/2}$ and F-*KLL* diffractograms were measured for some films.

Throughout Secs. III and IV the reader must be conscious of XPS and XPD being surface sensitive techniques. For electron kinetic energies relevant in the present study, i.e., the 560–1100 eV regime, the elastic mean free path varies from 5.3 to 7.5 monolayers. Thus in the case of Y(0001) ($c = 5.73$ Å) the elastic mean free path varies from 15 to 22 Å. In Table I and in the following discussion we use cross section corrected F 1*s* to Y 3*d*, C 1*s* to Y 3*d*, and O 1*s* to Y 3*d* intensity ratios. Note that only films A (550 Å at 700 °C) and E (500 Å at RT, 5×10^{-6} mbar H_2) were grown on bare CaF_2(111) substrates. After the deposition of these films the Ca 2*p* doublet was no longer detectable, i.e., the substrate was completely covered, and no O or C contaminations could be detected with XPS. Film B was deposited on top of film A (+250 Å, 350 °C), and film C on top of the slightly oxygen contaminated film B (+200 Å, RT). Films D and F, finally, correspond to film C annealed to 700 °C and to film E annealed to 600 °C, respectively.

In the case of film A (550 Å) the XPS spectra were shifted toward lower kinetic energies by ≈2 eV, whereas no charging effects could be detected for thicker (≥ 800 Å) Y films (films B, C, and D). Above a critical film thickness of ≈ 800 Å the Y films seem to be in electrical contact with the grounded sample holder. Note that in Figs. 2 and 5 the spectra taken from film A have been shifted manually to correct for this charging effect. In the case of the 500 Å thick films

TABLE I. Summary of the preparation procedure for each film, as well as the respective results obtained from LEED, XPD, and XPS line shape and peak position analysis. The labels *V* and *S* assign two different components of the F 1*s* emission (see Fig. 2).

					Int. relative to Y 3*d* (%)			
			LEED (arbitrary	Fluoride component	F 1*s*			
Film	Preparation	XPD	judged LEED quality)	in Y 3*d* emission	*V*+*S*	*V*	*S*	O 1*s*
A	550 Å, 700 °C		sharp (3)	yes	14.3	9.0	5.3	0.0
B	+250 Å, 350 °C	hcp(0001)	broad (2)	yes	13.2	9.8	3.5	0.6
	70° off normal				23.4	9.0	14.0	1.0
	after XPD (20 h)							4.9
C	+200 Å, RT		diffuse (1)	?	5.7	3.9	1.8	1.7
D	annealed 700 °C		very sharp (4)	no	13.0	0.0	13.0	0.2
E	500 Å, RT, under 5×10^{-6} mbar H_2	fcc(111)	no spots (0)	no	0.0	0.0	0.0	0.0
F	annealed 600 °C	hcp(0001)	very sharp (4)	no	8.5	0.0	8.5	0.9

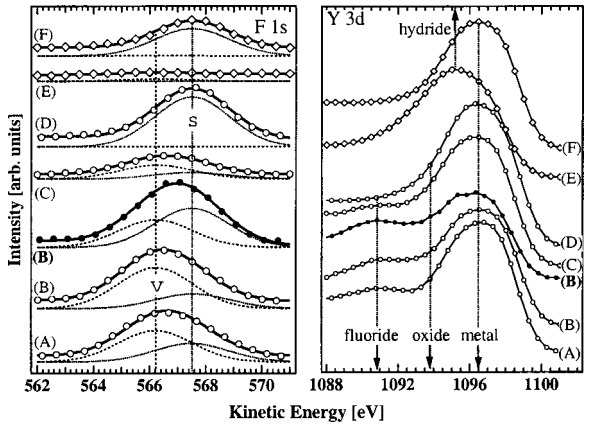

FIG. 2. XPS spectra illustrating peak positions and line shapes of the F 1*s* singlet and the Y 3*d* doublet for the different Y films (see Table I for preparation conditions). The open and filled — a 70° off-normal measurement taken from film B — circles are the data. In the case of the F 1*s* emission, the solid curves are the best fits to the data using two Gauss functions (dashed and dotted curves). For the Y 3*d* emission the solid lines are just a guide for the eye. The arrows indicate the peak position of the Y 3*d* doublet for Y in different chemical environments.

E and F on the other hand energy shifts due to charging effects were avoided as follows: prior to deposition of film E small Au contacts were first evaporated on each corner of the platelets leaving the center area ($\varnothing \approx 8$ mm) of the $CaF_2(111)$ surface uncovered from Au. Care was taken that the Au contacts were in contact with the electrically grounded sample holder. Then, Y was deposited on top of both the Au contacts and the bare center area of the CaF_2 platelets, i.e., the resulting Y films were electrically grounded. Indeed, no energy shifts due to charging effects were observed in the respective XPS spectra (Figs. 2 and 5).

III. RESULTS AND DISCUSSION

XPS spectra taken from the untreated $CaF_2(111)$ substrates are shown in Fig. 1(a). Besides the characteristic Ca and F core level and Auger lines, the spectrum showed 20% O 1*s* (cross section corrected O 1*s* to F 1*s* intensity ratio) and 48% C 1*s* (cross section corrected C 1*s* to F 1*s* intensity ratio) lines. By heating the $CaF_2(111)$ substrates during 30 min to 700 °C the carbon contamination could be reduced below the limit of detectability of XPS, while the oxygen contamination was reduced to 3% [Fig. 1(b)]. Moreover, both the Ca 2*p* doublet and F 1*s* singlet photoemission lines broaden and shift toward lower kinetic energies, indicative of a second set of peaks at $\approx$ 1.5 and 1.2 eV lower kinetic energies, respectively.

It is known that CaF_2 cleaves along the (111) plane between two adjacent fluorine layers, resulting in a fluorine-terminated surface.[45–50] In connection with the following Y spectra and their discussion, the question of termination of the ''clean,'' i.e., the annealed $CaF_2(111)$ substrate [see Fig. 1(b)] is of interest. Assuming stoichiometric CaF_2 we have calculated the expected intensity ratios between the Ca 2*p* and F 1*s* emission for the sequences from the surface CaFF..., FCaF..., and FFCa... as a function of the average interlayer distance.[51] The experimental Ca 2*p* to F 1*s* ratio of 1.1 obtained for the clean substrate [Fig. 1(b)] is only compatible with a Ca termination. A Ca rich surface termination could be caused by fluorine desorption at high temperatures, a scenario that requires high mobility of fluorine in the Ca lattice. Electrical conductivity data support this speculation: the electrical conductivity of CaF_2 is exclusively ionic, and it is related to the motion of fluorine ions and vacancies through the Ca lattice, a process which is known to be effective only at sufficiently high temperatures ($\geqslant 500$ °C).[52,53] Furthermore, it is known that fluorine desorption from CaF_2 can be stimulated by photon[45] and electron[46–50] irradiation by the Knotek–Feibelmann[54] mechanism or via exciton formation.[55] We therefore expect fluorine to further desorb and, hence, the Ca content at the surface to further increase during XPS and XPD experiments, i.e., when irradiating the $CaF_2(111)$ sample with photons ($h\nu = 1253.6$ eV) and photoelectrons ($E_{kin} \leqslant 1253.6$ eV) under UHV conditions. Comparison of Fig. 1(b) (the first spectrum from the annealed sample) with Fig. 1(c) (XPS spectra measured after a 20 h XPD experiment) shows that this is the case: the Ca 2*p* to F 1*s* ratio increased by $\approx$20%! Now the original high-kinetic energy set of F and Ca lines is considerably reduced or even absent. The intensity of the O 1*s* line in turn increased to 16% and the broad peak indicates a component at higher kinetic energies. We therefore relate the remaining low-kinetic energy Ca peaks to oxidized Ca clusters on the surface. This interpretation is consistent with the oxidation of Ca clusters formed by electron stimulated decomposition of air cleaved CaF_2 crystals under UHV conditions.[47–50,56] Since the surface is depleted from F after the XPD experiment, we attribute the low-kinetic energy F 1*s* singlet to fluorine located in deeper layers, while the original F 1*s* singlet appears to be caused by fluorine located at the surface.

Figure 2 shows the photoemission intensity (open circles, the filled circles are a 70° off-normal measurement taken from film B) in the region of the F 1*s* singlet and the Y 3*d* doublet. Note that due to the Au contacts (see Sec. II) no energy shifts due to charging effects were observed for these spectra. For the 550 Å thick Y film grown at 700 °C (film A), i.e., the growth temperature used in the study by Nagengast *et al.*,[34] LEED yields a sharp hexagonal pattern (not shown). This is consistent with the previously reported growth of single-crystalline hcp(0001) oriented Y films on $CaF_2(111)$.[34] The sharp LEED reflexes reveal a well-ordered surface. Since the Ca 2*p* doublet could not be detected we conclude that the substrate is completely covered with Y. The surprisingly intense F 1*s* singlet (14.3%) reveals the presence of fluorine in the near surface region [Fig. 2(A)]. Since we never observed F contaminations for Y films grown on W(110) or Nb(110) in the same UHV system and under the same deposition conditions,[24–26,42] we conclude that the fluorine cannot originate from the residual gas. Consequently, it must originate from the $CaF_2(111)$ substrate.

Aiming at well-ordered, fluorine free Y films, we gradually lowered the substrate temperature during Y deposition in a first series of experiments. To this goal additional Y films were deposited on top of film A. After the addition of 250 Å Y at 350 °C (film B) only very little changes are visible in

the XPS spectra [Fig. 2(B)]. In particular, the fluorine concentration is only reduced by 1%. Moreover, the LEED reflexes are already somewhat broader than for film A. 20 h later (used for XPD) we made an additional deposition of 200 Å Y at RT (film C) on top of film B, which was by then contaminated with 4.9% oxygen. As a result, the intensity of both the oxygen and the fluorine line reduced by a factor of ≈ 3. The diffuse LEED reflexes indicated a poorly ordered surface for film C. A highly ordered surface could be restored by annealing film C to 700 °C (film D). However, the corresponding XPS spectrum [Fig. 2(D)] shows that this procedure also restores the F 1*s* singlet (13%), while the oxygen line is considerably reduced or even absent.

In previous work we have demonstrated that for Y deposition on W(110) without H_2 sharp LEED patterns could only be observed for temperatures above ≈ 550 °C. In contrast, Y deposition on W(110) under a H_2 partial pressure of $\approx 5 \times 10^{-6}$ mbar yields sharp LEED patterns for substrate temperatures ranging from RT up to 330 °C.[24–26] This suggests direct Y dihydride growth, i.e., Y deposition under a H_2 partial pressure of $\approx 5 \times 10^{-6}$ mbar at RT to be a promising way to grow well-ordered, fluorine free Y (hydride) films on $CaF_2(111)$. In a second series of experiments we therefore deposited 500 Å Y on a clean $CaF_2(111)$ substrate under a H_2 partial pressure of $\approx 5 \times 10^{-6}$ mbar at RT (film E). Most importantly, no fluorine could be detected with XPS for this surprisingly transparent film of a red/yellow color [Fig. 2(E)]. However, as revealed by the absence of LEED reflexes and the poorly defined XPD pattern (not shown) film E is unfortunately of very poor crystallinity. The XPD data can be explained with a fcc(111) oriented Y lattice. In order to recover good crystallinity, we finally annealed film E by gradually increasing the temperature under simultaneous observation of the LEED screen. At about 600 °C LEED reflexes reappeared, the film lost its transparency, and became a shiny metallic α-phase film (film F). However, the XPS spectra taken immediately afterward [Fig. 2(F)] show all the features discussed earlier for film D. In particular, XPS detects 8% fluorine and XPD reveals a hcp(0001) oriented Y film (not shown).

So far, all our XPS and LEED results indicate that the growth of well-ordered single crystalline Y films on $CaF_2(111)$ is inseparable from the occurrence of fluorine. For RT deposition we observe disordered surfaces with no or little fluorine contamination. With increasing deposition and/or annealing temperature, both the surface quality and the fluorine contamination increase. The intriguing question is whether there is a chemical reaction between Y and F leading to compound formation through the whole film or whether F is dominantly located at the surface.

A first indication for preferential location of F at the surface emerges from x-ray photoelectron diffraction from film B (Fig. 3). The Y $3d_{5/2}$ diffractogram [Fig. 3(a)] reveals sixfold symmetry. An identical pattern was observed for 200 Å Y deposited at RT on W(110) or on Nb(110) and was identified as a single-crystalline hcp(0001) oriented Y film.[24–26,42] The F-*KLL* Auger emission pattern [Fig. 3(a)] in contrast is rather diffuse. It shows six-fold symmetry around the F emitters and exhibits a forward focusing maxima along

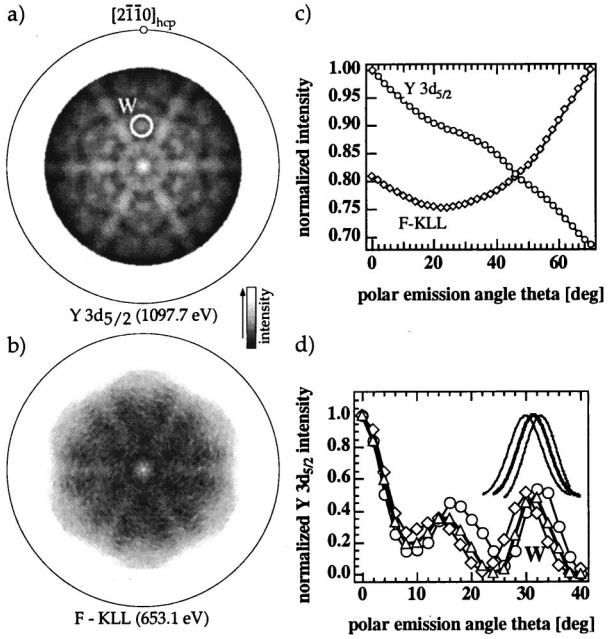

FIG. 3. Stereographic projection of experimental: (a) Y $3d_{5/2}$ photoelectron and (b) F-*KLL* Auger intensities from film B, (c) azimuthally averaged intensity as a function of the polar emission angle Θ for Y $3d_{5/2}$ (open circles) and F-*KLL* (open diamonds) emission from film B, and (d) polar cut through the prominent forward-scattering maxima *W* for film B (open triangles), a 200 Å thick Y film on W(110) (open circles), and a 200 Å thick Y trihydride film on W(110) (open diamonds). The polar angle position of *W* (Θ_W) was determined by fitting the data with a Gauss function.

normal emission. This clearly indicates that F atoms are present below the surface. The presence of fluorine atoms at the surface is unveiled by azimuthally averaged intensity curves [Fig. 3(c)]. While the azimuthally averaged Y $3d_{5/2}$ intensity (open circles) shows the behavior expected for a thick film or bulk sample, the increasing azimuthally averaged F-*KLL* intensity (open diamonds) with increasing polar emission angle Θ is typical for atoms adsorbed on or within the surface layer.

Further evidence pf a preferential location of F at the surface emerges from line shape and peak position analysis of the F 1*s* singlet and Y 3*d* doublet. The linewidth and the line shape of the F 1*s* emission from films A, B, and C are rather broad (≈ 3.4 eV FWHM) and slightly asymmetric (Fig. 2). For films D and F the linewidth is reduced (≈ 3.0 eV FWHM) and the line shape is almost symmetric. Furthermore, the F 1*s* peak position shifts toward higher kinetic energies, when going from films A, B, and C to films D and F. These observations suggest the presence of two F 1*s* singlets, in the following labeled *V* and *S*. We estimated the intensities of *V* and *S* (see Table I) by fitting the data with two Gauss functions (solid curves in Fig. 2). The best fits were achieved for a peak separation of 1.2 eV and a linewidth of 3 eV FWHM. Interestingly, the presence of the F 1*s* *V* singlet goes along with the presence of a shoulder in the Y 3*d* emission at ≈ 6 eV lower kinetic energies. A shift of 6 eV with respect to the Y 3*d* metal component cannot be explained by an oxide or a hydride. For Y_2O_3, $YH_{2.99}$, and $YH_{2.25}$ films we previously measured shifts of 2.5 eV,[42] 1.9 eV,[26] and 0.6 eV,[26] respectively. However, a shift of ≈ 6 eV

is comparable to bulk values of YF_3.[57] Furthermore, the peak position of the F 1*s* *V* component coincides fairly well with the peak position expected for F 1*s* emission from YF_3 bulk. This indicates that the shoulder at ≈6 eV lower kinetic energy in the Y 3*d* emission and, consequently, the F 1*s* *V* component are due to fluoride formation. A 70° off-normal emission measurement of film B [filled circles in Fig. 2(B)] supports this interpretation. While the intensity of the F 1*s* *V* component remains almost constant when going from normal to off-normal emission, the intensity of the F 1*s* *S* component increases by a factor of 3. Obviously, the F 1*s* *S* component is due to F atoms floating at the surface while, in good agreement with the XPD analysis above, the F 1*s* *V* component is caused by F atoms below the surface.

It is noteworthy that annealing after the deposition (film C → film D and film E → film F) causes the F 1*s* *V* component to vanish completely, while the F 1*s* *S* component gains in intensity. Obviously fluorine surface segregation dominates the release of fluorine from the CaF_2 substrate, thereby preventing a fluoridation of the whole Y film. Furthermore, the sequence of film A, B, and C reveals that the intensity of the F 1*s* *S* component gradually reduces, while the intensity of the F 1*s* *V* component remains constant when going from film A to film B and only reduces when going from film B to film C. Apparently an additional mechanism competing surface segregation is active during Y deposition: fluorine atoms floating on the surface can become buried by incoming Y atoms. As a result fluorine cannot be eliminated from subsurface regions and hence causes the observation of the F 1*s* *V* component during Y deposition.

The formation of a well-ordered surface requires mass transport at the surface. Often, an increased mass transport can simply be achieved upon annealing and/or growth at higher substrate temperatures. An alternative possibility to affect mass transport and, hence, the quality of the surface, is the use of additives present on the surface, so-called surfactants. Having evidence that for Y films exhibiting sharp LEED patterns a significant part of the fluorine is concentrated at the surface, the question arises, whether the surface quality is determined by deposition or postdeposition annealing temperatures alone, or also by F on the surface playing the role of a surfactant.

LEED images have been judged for their quality and marked in arbitrary units from 4 (sharpest spots) to 0 (no spots) (see Table I). Figure 4 displays the LEED (surface) quality as a function of temperature [Fig. 4(a)], the F 1*s* intensity [Fig. 4(b)], the intensity of the F 1*s* *V* component [Fig. 4(c)], and the intensity of the F 1*s* *S* component [Fig. 4(d)]. The filled circles represent films that have been annealed after deposition, while the plus signs stand for the Y films deposited at different substrate temperatures. The correlation between the LEED quality and the F 1*s* and F 1*s* *V* component is rather bad. Since the temperature and the F 1*s* *S* component are directly related to each other via surface segregation, these two quantities cannot be separated definitely. Nevertheless, the fact that the LEED quality correlates even better with the intensity of the F 1*s* *S* component than with temperature alone is a strong indication that, in addition to temperature-driven mass transport, surfactant action of

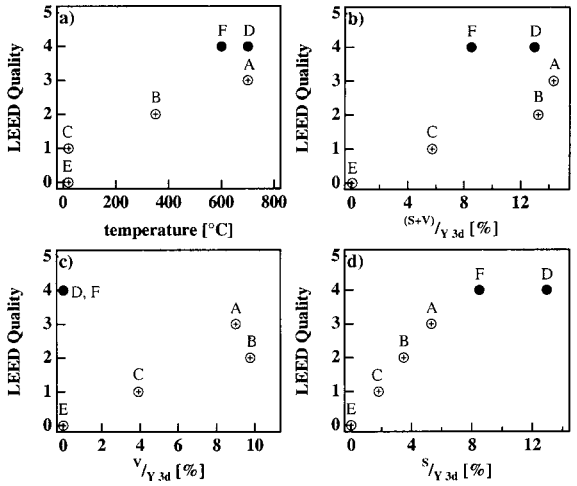

FIG. 4. LEED (surface) quality (see Table I for assignments) as a function of the: (a) deposition or annealing temperature, (b) the F 1*s* intensity, (c) the intensity of the F 1*s* *V* component, and (d) the intensity of the F 1*s* *S* component. The filled circles represent films that have been annealed after deposition, while the plus signs stand for the Y films deposited at different substrate temperatures.

fluorine further enhances mass transport of Y atoms at the surface.

The definite separation of the temperature effect from surfactant action of fluorine would require us to grow Y on fluorine free substrates, and then to dose fluorine either before, during, or after the Y deposition. It is obvious that this is an experiment nobody likes to carry through in an UHV system. This may be part of the reason why surfactant action of fluorine has not been reported so far.[58] Surfactant action of other metaloids such as O and H, however, is widespread. Clear evidence of surfactant action of fluorine would therefore not be too surprising.

In a previous study, based on XPD analysis and thermodynamic considerations, we found that the H concentration of Y films deposited on W(110) under a H_2 partial pressure of $\approx 5\times10^{-6}$ mbar at RT corresponds to the lower boundary of the pure dihydride phase ($x\approx1.99$).[24–26] Both $YH_{1.99}$ and the stoichiometric β phase compound YH_2 have a high electrical conductivity and optical absorption.[4,8] For Y deposition on $CaF_2(111)$ under a H_2 partial pressure of $\approx 5\times10^{-6}$ mbar at RT (film E), we consequently expected to observe an optically absorbing film. Surprisingly, film E is a transparent film of red/yellow color.

Measurements with increased resolution (as compared to the ones in Fig. 2) of the energy region of the Y 3*d* emission (Fig. 5) give an indication why film E is transparent. The spectrum of film E shows a larger intensity for the peak at lower kinetic energy (≈1095 eV) corresponding to the $3d_{3/2}$ emission than for the peak reflecting $3d_{5/2}$ emission [Fig. 5(E)]. Such a behavior is opposed to the observation of films grown under the same partial pressure of hydrogen on tungsten yielding a H concentration of $x=1.99$ [Fig. 5($YH_{1.99}$)], but is in agreement with a film of composition $YH_{2.25}$ [Fig. 5($YH_{2.25}$)], which was obtained by exposing an $YH_{1.99}$ film grown on tungsten to a hydrogen pressure of 100 mbar for 4 min.[25,26] At a H:Y ratio of 2.25 the phase diagram indicates a mixture of the β and γ phase. Using the model described in

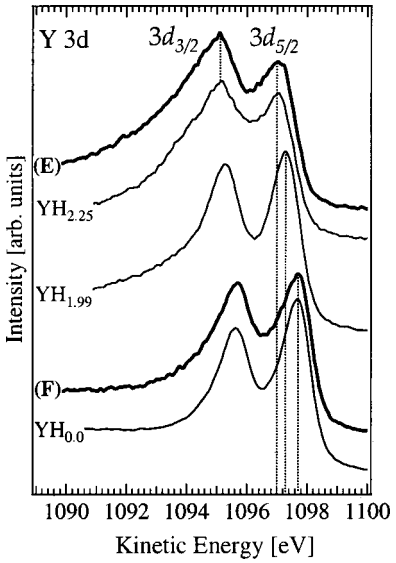

FIG. 5. XPS spectra illustrating peak positions and line shape of the Y $3d$ doublet. (Film E) 500 Å deposited on $CaF_2(111)$ at RT under a H_2 partial pressure of $\approx 5\times10^{-6}$ mbar. (Film F) Film E annealed to 600 °C. Note, that due to the Au contacts (see Sec. II) no charging effects are observed for films E and F. ($YH_{0.0}$ film) 200 Å thick Y film deposited on W(110) at 330 °C. ($YH_{1.99}$ film) 200 Å thick Y film deposited on W(110) at RT under a H_2 partial pressure of $\approx 5\times10^{-6}$ mbar. ($YH_{2.25}$ film) A $YH_{1.99}$ film grown on tungsten after exposure to a hydrogen pressure of 100 mbar for 4 min.

Refs. 25 and 26 to estimate the hydrogen concentration from the relative intensities of the $3d_{3/2}$ and $3d_{5/2}$ emission, film E has a hydrogen concentration of 2.3. For this value, 25% of the sample is in the yellowish transparent γ phase and 75% is in the absorbing red β phase. After annealing film E to 600 °C the Y $3d$ doublet is shifted by ≈ 0.6 eV toward higher kinetic energies [Fig. 5(F)]. Moreover, the line shape is very similar to the Y $3d$ doublet obtained from a clean Y film grown on W(110) [Fig. 5($YH_{0.0}$)]. Obviously, hydrogen could be unloaded successfully from the Y hydride films.

It is not yet clear what causes the different hydrogen concentrations for Y films grown on $CaF_2(111)$ ($x\approx 2.3$) and W(110) ($x\approx 1.99$) under a H_2 partial pressure of $\approx 5\times10^{-6}$ mbar. One argument may be of chemical or thermodynamic nature. For example, fluorine atoms — initially those of the bare $CaF_2(111)$ substrate, later on those floating on the growing Y hydride film — may catalyze the H_2 dissociation and thereby promote the hydrogen absorption. Since contrary to the direct dihydride growth on W(110) surfaces, LEED reflexes were not found for the Y hydride film grown on $CaF_2(111)$ surface, disorder might also play a role. As discussed in the following, the Y $3d_{5/2}$ diffractogram taken from film B [Fig. 3(a)] indicates a third possibility. The polar emission angle Θ_W of the prominent forward scattering maxima labeled W is a very direct measure of the c/a ratio in hcp(0001) lattices [$\tan(\Theta_W)=a/c$]. Figure 3(d) shows, that the c/a ratio of film B (open triangles) is inbetween those of 200 Å thick Y (open circles) and Y trihydride (open diamonds) films on W(110). Using basal plane lattice parameters determined by LEED and x-ray scattering,[34] we find that the c-axis lattice constant of the 200 Å thick Y film on W(110) equals the value for Y bulk, while the c-axis lattice constant of film B is expanded by 4.2% compared to bulk Y (see Table II). This 4.2% c-axis lattice constant expansion in film B compares closely to the H induced 4.5% perpendicular interplane distance expansion when going from α to β in bulk Y,[1] and in epitaxial Y films grown on Nb(110).[32] In particular, it is known that upon H loading the perpendicular interplane distance expands gradually, while the basal plane lattice parameter remains almost constant.[1,32,59] In turn, an expanded perpendicular interplane distance of a growing Y film may, compared to a relaxed film, favor hydrogen incorporation during deposition and, hence, yield a higher H concentration.

Although smaller, an expanded c-axis lattice constant for Y films on $CaF_2(111)$ grown at 700 °C was also reported in Nagengast *et al.*'s x-ray scattering study:[34] while for 3000 Å thick films the expansion amounts to only 0.2%, the c-axis lattice constant of 240 Å thick films is expanded by 1.5%. At present it is not clear why the c-axis lattice constant of Y films grown on $CaF_2(111)$ is significantly larger than that of Y bulk or Y films grown on W(110). Hydrogen incorporation during deposition cannot cause such a large lattice expansion. Furthermore, unless assuming that the H_2 dissociation is favored by the presence of fluorine, this scenario cannot account for the differences observed for deposition on different substrates. Lattice mismatch causing strain at the substrate–film interface certainly affects the initial growth and the film lattice near the interface. After the first stages of growth, however, films usually relax. Indeed, LEED[26] and

TABLE II. Relevant forward focusing maxima and lattice parameters for Y (hydride) bulk samples (from literature) as well as Y (hydride) films grown on $CaF_2(111)$ and W(110).

	Structure	Polar angle position of W (see Fig. 3) Θ_W(°)	c_{hcp}/a_{hcp}	In plane nearest neighbor distance a (Å)	Perpendicular interplanar distance (Å)	Expansion from Y bulk (%)
Y bulk[a]	hcp	—	1.57	3.65	2.87	0.0
Y/W(110)[b]	hcp	32.6	1.56	3.67	2.87	0.0
Y/CaF_2(111) (B)	hcp	31.5	1.63	3.67[34]	2.99	4.2
YH_2 bulk[a]	fcc	—	—	3.68	3.00	4.5
$YH_{2.9}$/W(110)[b]	hcp	29.8	1.75	3.71	3.24	12.9
YH_3 bulk[a]	hcp	—	1.81	3.68	3.33	16.0

[a]See Ref. 1.
[b]See Ref. 26.

x-ray scattering data[34] from Y/W(110) and Y/CaF_2(111) demonstrate that the basal plane lattice constant is relaxed in both systems. Finally, fluorine dissolved in the Y lattice could cause this unexpected large *c* axis. As can be seen from Fig. 2 and Table I Y deposition above $\approx 300\,^{\circ}$C yields a rather high fluorine contamination. As discussed above, XPS indicates that part of the fluorine concentrates at the surface. A fluorine induced lattice expansion would therefore be most pronounced near the surface, i.e., the region probed by XPD. This scenario is consistent with the different *c*-axis lattice constant expansions of 4.2% and 1.5% as referred from surface sensitive XPD and bulk-sensitive x-ray scattering[34] experiments, respectively.

IV. CONCLUSION

The epitaxial growth of Y and Y hydride films on CaF_2(111) has been investigated using XPS, XPD, and LEED. Good epitaxial growth is obtained for a substrate temperature of 700 °C. Most importantly we find that whenever the Y film showed good epitaxy, the surface was rich in fluorine. Only when the substrate temperature was chosen so low that the LEED reflexes were very broad was no fluorine detected with XPS (see Table I). Since fluorine impurities within the Y film and at its surface strongly affect the electronic structure and the mean free path of conduction electrons, this result is very important for the analysis of future electrical transport, optical transmission, and angle resolved photoemission experiments using high-quality epitaxial Y (hydride) films grown on CaF_2(111).

The observation that the surface quality correlates better with the surface fluorine concentration than with temperature (see Fig. 4) is a strong indication that fluorine acts as a surfactant. However, since fluorine surface segregation relates the fluorine surface concentration directly to the temperature, the surfactant action cannot be separated unequivocally from temperature-controlled mass transport on the surface.

For Y deposition without H_2 the Y atoms form a hcp(0001) oriented lattice. In contrast to Y films grown on W(110), XPD reveals that near the surface the *c*-axis lattice constant of Y films on CaF_2(111) is expanded by 4.2% compared to Y bulk (see Table II). At present it is not clear what causes this unusually big *c*-axis lattice expansion in Y films grown on CaF_2(111). It could be induced by fluorine solved in the Y lattice. Taking into account that Y is concentrated at the surface, this speculation is corroborated by the fact that bulk sensitive x-ray scattering measurements find a *c*-axis lattice constant expansion of only 1.5%.[34]

For Y deposition under a H_2 partial pressure of 5×10^{-6} mbar at RT a red–yellow transparent and fluorine free film of very poor crystallinity is obtained. Using a model based on line shape and peak position analysis of the Y $3d$ core level we find a H concentration of $x=2.3$, i.e., 25% of the samples are in the yellowish transparent γ phase and 75% are in the absorbing red β phase. Such a behavior is opposed to the observation of single crystalline dihydride films ($x=1.99$) grown under the same H_2 partial pressure on W(110).[24–26] The enhanced H incorporation for Y deposition under the same H_2 partial pressure on CaF_2(111) as compared to deposition on W(110) could be caused by the unusually big *c*-axis lattice expansion discussed above. Alternatively, fluorine atoms — initially those of the bare CaF_2(111) substrate, later on those floating on the growing Y hydride film — may catalyze the H_2 dissociation and thereby promote the hydrogen absorption.

Upon annealing the $YH_{2.3}$ film to 600 °C hydrogen unloads and Y lattice transforms from a poorly ordered fcc(111) into a highly ordered hcp(0001) oriented lattice. Thereby the film loses its transparency and becomes a shiny metallic α-phase film. At the same time fluorine contamination is restored. This route is therefore not practical to produce fluorine-free high-quality epitaxial Y films.

ACKNOWLEDGEMENTS

Skillful technical assistance was provided by F. Bourqui, Ch. Neururer, E. Mooser, R. Schmid, and O. Raetzo. This project was supported financially by the Fonds National Suisse pour la Recherche Scientifique and by the TMR Research Network ''Switchable metal hydride films.''

[1] P. Vajda, in *Handbook on the Physics and Chemistry of Rare Earths*, edited by K. A. Gschneider and L. Eyring (Elsevier, Amsterdam, 1995), Vol. 20, and references therein.
[2] A. Fujimori and L. Schlapbach, J. Phys. C **17**, 341 (1984).
[3] J. Osterwalder, Z. Phys. B: Condens. Matter **61**, 113 (1985).
[4] J. N. Huiberts, R. Griessen, J. H. Rector, R. J. Wijngaarden, J. P. Dekker, D. G. de Groot, and N. J. Koeman, Nature (London) **380**, 231 (1996).
[5] R. Griessen, J. N. Huiberts, M. Kremers, A. T. M. van Gogh, N. J. Koeman, and P. H. L. Notten, J. Alloys Compd. **253–254**, 44 (1997).
[6] P. H. L. Notten, M. Kremers, and R. Griessen, J. Electrochem. Soc. **143**, 3348 (1996).
[7] R. Griessen, Phys. Bl. **53**, 1207 (1997).
[8] M. Kremers, N. J. Koeman, R. Griessen, P. H. L. Notten, R. Tolboom, P. J. Kelly, and P. A. Duine, Phys. Rev. B **57**, 4943 (1998).
[9] P. van der Sluis, M. Ouwerkerk, and P. A. Duine, Appl. Phys. Lett. **70**, 3356 (1997).
[10] J. P. Dekker, J. van Ek, A. Lodder, and J. N. Huiberts, J. Phys.: Condens. Matter **5**, 4805 (1993).
[11] Y. Wang and M. Y. Chou, Phys. Rev. Lett. **71**, 1226 (1993).
[12] Y. Wang and M. Y. Chou, Phys. Rev. B **51**, 7500 (1995).
[13] P. J. Kelly, J. P. Dekker, and R. Stumpf, Phys. Rev. Lett. **78**, 1315 (1997).
[14] R. Ahuja, B. Johansson, J. M. Wills, and O. Eriksson, Appl. Phys. Lett. **71**, 3498 (1997).
[15] T. J. Udovic, Q. Huang, and J. J. Rush, Phys. Rev. Lett. **79**, 2920 (1997).
[16] P. J. Kelly, J. P. Dekker, and R. Stumpf, Phys. Rev. Lett. **79**, 2921 (1997).
[17] H. Kierey, M. Rode, A. Jacob, A. Borgschulte, and J. Schoenes, Phys. Rev. B **63**, 134109 (2001).
[18] A. T. M. van Gogh, E. S. Kooij, and R. Griessen, Phys. Rev. Lett. **83**, 4614 (1999).
[19] K. K. Ng, F. C. Zhang, V. I. Anisimov, and T. M. Rice, Phys. Rev. Lett. **78**, 1311 (1997).
[20] R. Eder, H. F. Pen, and G. A. Sawatzky, Phys. Rev. B **56**, 10 115 (1997).
[21] K. K. Ng, F. C. Zhang, V. I. Anisimov, and T. M. Rice, Phys. Rev. B **59**, 5398 (1999).
[22] T. Miyake, F. Aryasetiawan, H. Kino, and K. Terakura, Phys. Rev. B **61**, 16 491 (2000).
[23] P. van Gelderen, P. A. Bobbert, P. J. Kelly, and G. Brocks, Phys. Rev. Lett. **85**, 2989 (2000).
[24] J. Hayoz, S. Sarbach, Th. Pillo, E. Boschung, D. Naumović, P. Aebi, and L. Schlapbach, Phys. Rev. B **58**, R4270 (1998).
[25] J. Hayoz, Ph.D. thesis, University of Fribourg, 1999.
[26] J. Hayoz, Th. Pillo, M. Bovet, A. Züttel, St. Guthrie, G. Pastore, L. Schlapbach, and P. Aebi, J. Vac. Sci. Technol. A **18**, 2417 (2000).
[27] S. J. van der Molen, J. W. J. Kerssemakers, J. H. Rector, N. J. Koeman, B. Dam, and R. Griessen, J. Appl. Phys. **86**, 6107 (1999).
[28] M. Rode, H. Kierey, A. Jacob, U. Barkow, and J. Schoenes, Verh. Dtsch. Phys. Ges. **35**, 446 (2000).

[29] B. Hjörvarsson *et al.*, J. Phys.: Condens. Matter **11**, L119 (1999).
[30] J. Hayoz, Th. Pillo, M. Bovet, L. Schlapbach, and P. Aebi (unpublished).
[31] A. Remhof, G. Song, K. Theis-Bröhl, and H. Zabel, Phys. Rev. B **56**, R2897 (1997).
[32] A. Remhof, G. Song, Ch. Sutter, A. Schreyer, R. Siebrecht, H. Zabel, F. Güthoff, and J. Windgasse, Phys. Rev. B **59**, 6689 (1999).
[33] A. Remhof, G. Song, Ch. Sutter, D. Labergerie, M. Hübner, H. Zabel, and J. Härtwig, Phys. Rev. B **62**, 2164 (2000).
[34] D. G. Nagnegast, J. Kerssemakers, A. T. M. van Gogh, B. Dam, and R. Griessen, Appl. Phys. Lett. **75**, 1724 (1999).
[35] A. Jacob, A. Borgschulte, and J. Schoenes, Verh. Dtsch. Phys. Ges. **35**, 430 (2000).
[36] C. S. Fadley, in *Synchrotron Radiation Research: Advances in Surface Science*, edited by R. Z. Bachrach (Plenum, New York, 1990), Vol. 1.
[37] P. Aebi *et al.*, Surf. Sci. **402–404**, 614 (1998).
[38] J. Osterwalder, P. Aebi, R. Fasel, D. Naumović, P. Schwaller, T. Kreutz, L. Schlapbach, T. Abukawa, and S. Kono, Surf. Sci. **331–333**, 1002 (1995).
[39] R. Fasel, P. Aebi, R. G. Agostino, D. Naumović, J. Osterwalder, A. Santaniello, and L. Schlapbach, Phys. Rev. Lett. **76**, 4733 (1996).
[40] J. Hayoz, D. Naumović, R. Fasel, P. Aebi, and L. Schlapbach, Surf. Sci. **373**, 153 (1997).
[41] J. Hayoz, Th. Pillo, R. Fasel, L. Schlapbach, and P. Aebi, Phys. Rev. B **59**, 15 975 (1999).
[42] J. Hayoz, M. Bovet, Th. Pillo, L. Schlapbach, and P. Aebi, Appl. Phys. A: Mater. Sci. Process. **71**, 615 (2000).
[43] D. Gregory and M. Fink, At. Data Nucl. Data Tables **14**, 39 (1974).
[44] The reported kinetic energies for F $1s$ and Ca $2p_{3/2}$ excited by Mg $K\alpha$ radiation in CaF_2 are 569 and 905.8 eV, respectively [see *Handbook of X-ray Photoelectron Spectroscopy*, edited by C. D. Wagner, W. M. Riggs, L. E. Davis, J. F. Moulder, and G. E. Muilenberg (Perkin-Elmer Corporation, Eden Prairie, MN, 1978)].
[45] U. O. Karlsson, F. J. Himpsel, J. F. Morar, F. R. McFeely, D. Rieger, and J. A. Yarmoff, Phys. Rev. Lett. **57**, 1247 (1986).
[46] M. Batzill and K. J. Snowdown, Appl. Phys. Lett. **77**, 1955 (2000).
[47] M. Reichling, R. M. Wilson, R. Bennewitz, R. T. Williams, S. Gogoll, E. Stenzel, and E. Matthias, Surf. Sci. **366**, 531 (1996).
[48] M. Huisinga, M. Reichling, and E. Matthias, Phys. Rev. B **55**, 7600 (1997).
[49] M. Reichling, M. Huisinga, D. Ochs, and V. Kempter, Surf. Sci. **404–404**, 145 (1998).
[50] R. Bennewitz, D. Smith, and M. Reichling, Phys. Rev. B **59**, 8237 (1999).
[51] The interlayer distance is used to calculate the elastic mean free path of the photoelectrons [see M. P. Seah and W. A. Dench, Surf. Interface Anal. **1**, 2 (1979)].
[52] *Crystals with the Fluoride Structure*, edited by W. Hayes (Oxford University Press, London, 1974).
[53] R. W. Ure, J. Chem. Phys. **26**, 1363 (1957).
[54] M. L. Knotek and P. Feibelman, Phys. Rev. Lett. **40**, 964 (1978).
[55] K. S. Song and R. T. Williams, in *Self-Trapped Excitons*, Springer Series in Solid-State Sciences (Springer, Berlin, 1996), Vol. 105.
[56] C. L. Strecker, W. E. Moddeman, and J. T. Grant, J. Appl. Phys. **52**, 6921 (1981).
[57] When going from bulk Y_2O_3 to bulk YF_3 the Y $3d$ emission shifts toward lower kinetic energies by 3.4 eV [see *Handbook of X-ray Photoelectron Spectroscopy*, edited by C. D. Wagner, W. M. Riggs, L. E. Davis, J. F. Moulder, and G. E. Muilenberg (Perkin-Elmer Corporation, Eden Prairie, MN, 1978)].
[58] H. Zabel (private communications).
[59] T. J. Udovic, Q. Huang, and J. J. Rush, J. Phys. Chem. Solids **57**, 423 (1996).